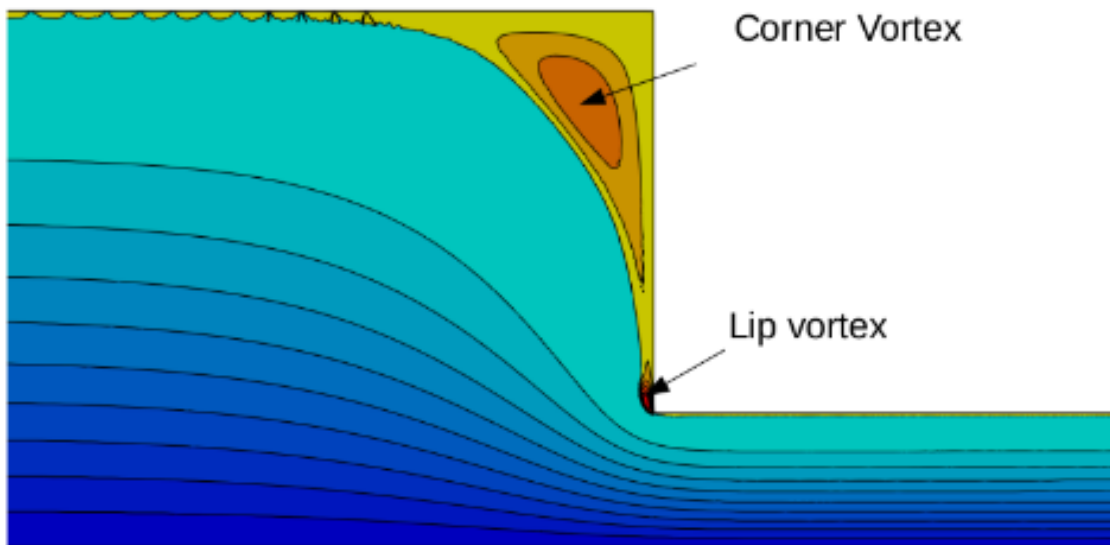




M2 MSIAM Master thesis
Numerical resolution of viscoelastic fluids. Simulation of a flow in abrupt contraction

Thomas El Jammal





Éditorial

Ce rapport est la concrétisation de la fin de mon cycle universitaire en Mathématiques appliquées que j'ai suivi à l'Université de Grenoble. Il m'a permis de mettre à l'épreuve mes connaissances acquises et ma capacité à les mettre en œuvre.

En raison de la pandémie de Covid-19, il a été réalisé en télétravail sous la tutelle de Pierre SARAMITO, directeur de recherches au CNRS à Grenoble. Je remercie vivement Pierre SARAMITO pour son écoute, son soutien sans faille dont il a fait preuve lors des visioconférences hebdomadaires que nous avons eu. Le télétravail a eu toutefois ses limites. Dans cet exercice isolé, je regrette de ne pas avoir eu l'expérience d'une atmosphère de travail plus sereine et d'un cadre de travail qui facilite les échanges avec les autres chercheurs du LJK.

Ce travail s'inscrit dans le domaine de la rhéologie, science de la matière en écoulement et recouvre des activités scientifiques majeures et se trouve associée à des technologies irremplaçables.

Contents

1	Introduction	2
2	The viscoelastic fluids equation	3
2.1	Equations of conservation	3
2.1.1	The mass conservation:	3
2.1.2	The momentum conservation:	3
2.1.3	Constitutive equation:	3
2.1.4	Constitutive equation for a viscoelastic fluid, the Oldroyd model:	4
3	Simulation in Abrupt Contraction:	6
3.1	The new formulation	6
3.1.1	Conformation tensor formulation	6
3.2	Logarithm of the conformation tensor formulation	7
3.2.1	The change of variable	7
3.2.2	The log derivative of a tensor	7
3.3	Abrupt contraction	12
3.3.1	Configuration	13
3.3.2	Simulations	16
4	Conclusion	21
A	Computation of special functions	22
A.1	Exponential of a tensor	22
A.2	Derivatives of the exponential of a tensor	22
A.3	Derivative of the function kappa	22
B	Computation of the stream function	22

1 Introduction

Rheology is the study of a material that have both a liquid and solid characteristics. It is at the frontier of solid and fluid mechanics enabling us to study a wide variety of materials. This report will be about the study of viscoelastic material flows. The study of viscoelastic fluids has started since the second half of the 20th century with the industrial production of molten and dilute polymers and the growth of engineering that generated many new product [7]. A material is said to be viscoelastic if it has both a viscous (liquid) and elastics (solid) behaviours, for instance polymers. The difficulty is to describe the macroscopic behaviour of a material that is composed microscopically of long and flexible polymers molecules suspended in a solvent. This special property set those materials in the non Newtonian fluids category leading to the modification of the constitutive equations from the Navier-Stoke problem.

To describe the macroscopic behaviour of a viscoelastic fluid, during the internship, we used the Oldroyd model. One of the main concerns about viscoelatic simulation was the Weissenberg number limitation, that has been treated in 2004 by Fattal and Kupferman [4]. By introducing a change of unknown, the authors allow the scientific community to rethink the existing algorithms and propose new methods to push further the simulation of viscoelastic flow at high Weissenberg number. In 2014, Pierre Saramito published an article [6] where a numerical method relying on Newton method allowed a direct steady numerical resolution of the problem.

In this report, we propose to do a direct application of the change of unknown to simulate a flow in abrupt contraction for a various number of Weissenberg using a Newton algorithm implemented in the open source library *Rheolef* [8]

2 The viscoelastic fluids equation

2.1 Equations of conservation

Let us introduce some useful notations and equations that will be used all along this report. The domain where the fluid flows will be denoted $\Omega \subset \mathbb{R}^3$, it will be an open set of the space. The density of a fluid will be denoted $\rho(t, x)$, it is a function of the space variable $x \in \Omega$ and of the time $t \geq 0$. The velocity of the fluid will be denoted $\mathbf{u}(t, x) = (u_i(t, x))_{1 \leq i \leq 3}$, it is a real valued function of the time variable $t \geq 0$ and of the space variable $x \in \Omega$. The velocity field will be denoted \mathbf{u} .

2.1.1 The mass conservation:

The first equation describing any fluid, Newtonian and non-Newtonian, is the conservation of mass. The mass conservation principle comes from the postulate that the mass of the fluid transported by the velocity field in the domain is conserved along the time. It can be written, for any subset $\nu(t) \subset \Omega$ for any $t \geq 0$:

$$\frac{d}{dt} \left(\int_{\nu(t)} \rho(t, \mathbf{x}) dx \right) = 0$$

This equation describe the mass conservation in non local form, but can be expressed locally instead of the arbitrary subdomain $\nu(t)$. Using some formula, that can be found in the book Complex Fluid [7], we can obtain the standard mass conservation in local form:

$$\rho \frac{\partial \rho}{\partial t} + \operatorname{div}(\rho \mathbf{u}) = 0 \quad (1)$$

In the rest of the report, we will use the hypothesis that the fluid is incompressible leading to the elimination of the $\frac{\partial \rho}{\partial t}$ because the density is constant.

2.1.2 The momentum conservation:

The momentum conservation is an equation that is verified by every fluid:

$$\rho \left(\frac{\partial \mathbf{u}}{\partial t} + (\mathbf{u} \cdot \nabla) \mathbf{u} \right) - \operatorname{div} \boldsymbol{\sigma}_{tot} = \rho \mathbf{g} \quad (2)$$

where $\boldsymbol{\sigma}_{tot}$ is the Cauchy stress tensor, and $(\mathbf{u} \cdot \nabla) \mathbf{u} = \left(\sum_{j=1}^3 u_j \frac{\partial u_i}{\partial x_j} \right)_{1 \leq i \leq 3}$.

2.1.3 Constitutive equation:

To describe the fluid, we now have a system of two equations, the mass and momentum conservation, with three unknown: the pressure p , the velocity field \mathbf{u} and the Cauchy stress tensor $\boldsymbol{\sigma}_{tot}$. Indeed, the system is not closed and we need to add relations between \mathbf{u} and $\boldsymbol{\sigma}_{tot}$ to close it. The difference between Newtonians and non-Newtonians fluids is in the relationship between \mathbf{u} and $\boldsymbol{\sigma}_{tot}$: for a Newtonian fluid, a linear relation between $\boldsymbol{\sigma}_{tot}$ and \mathbf{u} is enough to describe the behaviour of the fluid. For instance, writting:

$$\boldsymbol{\sigma}_{tot} = 2\eta D(\mathbf{u}) - \frac{2\eta}{3} \operatorname{div}(\mathbf{u}) \mathbf{I}$$

where $D(\mathbf{u})$ is the rate of deformation tensor, $D(\mathbf{u}) = \frac{1}{2}(\nabla\mathbf{u} + \nabla\mathbf{u}^T)$. Adding this equation to the mass and momentum conservation equations closes the system and we obtain the well known Navier-Stokes equations for a Newtonian fluid.

2.1.4 Constitutive equation for a viscoelastic fluid, the Oldroyd model:

The viscoelastic fluids do not have a unique model. Through my internship, we used the Oldroyd model.

A viscoelastic fluid has a viscous and elastic behaviour. Microscopically, polymer molecules are long flexible chains that can be approximated by a spring model. The main problem encountered in viscoelastic modelization is to describe at the macroscopic scale the behaviour of those microscopic polymer chains. To this end, we introduce the elastic stress tensor that will be denoted $\boldsymbol{\tau}$. This tensor verifies the following equation:

$$\frac{\dot{\boldsymbol{\tau}}}{\mu} + \frac{\boldsymbol{\tau}}{\eta_m} = 2D(\mathbf{u}) \quad (3)$$

where μ is the elastic modulus of the material at the macroscopic scale and η_m is the viscosity coefficient representing at the macroscopic scale the friction between polymer chains and the solvent molecules. $\dot{\boldsymbol{\tau}}$ is the lagrangian derivative

$$\dot{\boldsymbol{\tau}} = \frac{\partial\boldsymbol{\tau}}{\partial t} + (\mathbf{u}\cdot\nabla)\boldsymbol{\tau} \quad (4)$$

Let $\lambda = \eta_m/\mu$ be the relaxation time, last equation is rewritten as:

$$\lambda\dot{\boldsymbol{\tau}} + \boldsymbol{\tau} = 2\eta_m D(\mathbf{u}) \quad (5)$$

We can now introduce the cauchy stress tensor

$$\boldsymbol{\sigma}_{tot} = \boldsymbol{\tau} + 2\eta_s D(\mathbf{u}) - p\mathbf{I} \quad (6)$$

where η_s is the solvent viscosity, it represents the friction between solvent molecules. The problem of the lagrangian derivative of $\boldsymbol{\tau}$ 4 is that it depends on the frame of reference. To compensate that, Oldroyd introduced in 1950, the concept of the objective derivative of a tensor. In the complex fluid book [7], a whole section is dedicated to the building and computation of that derivative. We recall here the final result, to ensure the independence with respect to the frame of reference, we introduce the objective tensor derivative $\frac{D_a\boldsymbol{\tau}}{Dt}$:

$$\frac{D_a\boldsymbol{\tau}}{Dt} = \frac{\partial\boldsymbol{\tau}}{\partial t} + (\mathbf{u}\cdot\nabla)\boldsymbol{\tau} + \boldsymbol{\tau}W(\mathbf{u}) - W(\mathbf{u})\boldsymbol{\tau} - a(\boldsymbol{\tau}D(\mathbf{u}) + D(\mathbf{u})\boldsymbol{\tau}) \quad (7)$$

where $W(u)$ is the vorticity, given by $W(\mathbf{u}) = \frac{1}{2}(\nabla\mathbf{u} - \nabla\mathbf{u}^T)$ and a is a parameter belonging to $[-1; 1]$.

Finally, we can write the constitutive equation for any viscoelastic fluid under the Oldroyd

model:

$$\left\{ \begin{array}{ll} \operatorname{div} \mathbf{u} = 0 & \text{in }]0, T[\times \Omega \quad (8a) \\ \rho \left(\frac{\partial \mathbf{u}}{\partial t} + (\mathbf{u} \cdot \nabla) \mathbf{u} \right) - \operatorname{div}(\boldsymbol{\tau} + \eta_s D(\mathbf{u}) - p \mathbf{I}) = \rho \mathbf{g} & \text{in }]0, T[\times \Omega \quad (8b) \\ \lambda \frac{\mathcal{D}_a \boldsymbol{\tau}}{\mathcal{D}t} + \boldsymbol{\tau} = 2\eta_m D(\mathbf{u}) & \text{in }]0, T[\times \Omega \quad (8c) \\ \boldsymbol{\tau}(t=0) = \boldsymbol{\tau}_0 & \text{in } \Omega \quad (8d) \\ \mathbf{u}(t=0) = \mathbf{u}_0 & \text{in } \Omega \quad (8e) \\ \boldsymbol{\tau} = \boldsymbol{\tau}_\Gamma & \text{on }]0, T[\times \partial\Omega_- \quad (8f) \\ \mathbf{u} = \mathbf{u}_\Gamma & \text{on }]0, T[\times \partial\Omega \quad (8g) \end{array} \right.$$

where $\partial\Omega_- = \{x \in \partial\Omega; \mathbf{u}_\Gamma \cdot \mathbf{n}(x) < 0\}$ it is the upstream boundary, the inlet flow. We can see that boundary condition imposes \mathbf{u} on the whole boundary $\partial\Omega$ whereas only the upstream boundary $\partial\Omega_-$ is imposed for the tensor $\boldsymbol{\tau}$.

3 Simulation in Abrupt Contraction:

In this section, we simulate the flow of a viscoelastic fluid in abrupt contraction. This section is split in three subsections. First the reformulation of the viscoelastic problem 8 in term of the logarithm of the conformation tensor, the change of unknown proposed by Fattal and Kupfermann in [4]. The second part is the description of the configuration of the abrupt configuration and the last part is the comparison between the obtained result during the internship with the results obtained from the [5] article.

3.1 The new formulation

3.1.1 Conformation tensor formulation

The speed flow \mathbf{u} , the pressure field p and the elastic stress tensor $\boldsymbol{\tau}$ verify the system 8. The system is closed, we have 10 unknowns (6 in the elastic tensor, 3 in the velocity field and 1 in the pressure) and 1 scalar equation (1 in the mass conservation, 3 in the momentum conservation and 6 in the elastic transport equation).

To compute numerically the solution $\boldsymbol{\tau}$, the equation (3) has to be reworked by a change of variable. For a high Weissenberg number, the numerical computation of the viscoelastic fluids equations systemically fail. It seems that, at highly non linear singularities (at a corner or a border of an obstacle) of the domain, the norm become so high that it leads to numerical errors. In 2004, R.Fattal and R.Kupferman in [4] introduced a new formulation that involved logarithmic change of variable of the conformation tensor. In [6], in 2014, a new variant of the conformation tensor \mathbf{c} is introduced:

Let \mathbf{c} be the conformation tensor

$$\mathbf{c} = \boldsymbol{\tau} + \frac{\eta_m}{a\lambda} \mathbf{I}.$$

The problem is now expressed as follow.

Find $(\mathbf{u}, p, \mathbf{c})$ defined in $[0, T] \times \Omega$ such that:

$$\left\{ \begin{array}{ll} \operatorname{div} \mathbf{u} = 0 & \text{in }]0, T[\times \Omega \quad (9a) \\ \rho \left(\frac{\partial \mathbf{u}}{\partial t} + (\mathbf{u} \cdot \nabla) \mathbf{u} \right) - \operatorname{div}(\mathbf{c} + 2\eta_s D(\mathbf{u})) - \nabla p = \rho \mathbf{g} & \text{in }]0, T[\times \Omega \quad (9b) \\ \lambda \frac{\mathcal{D}_a \mathbf{c}}{\mathcal{D}t} + \mathbf{c} - \frac{\eta_m}{a\lambda} \mathbf{I} = 0 & \text{in }]0, T[\times \Omega \quad (9c) \\ \mathbf{c}(t = 0) = \mathbf{c}_0 & \text{in } \Omega \quad (9d) \\ \mathbf{u}(t = 0) = \mathbf{u}_0 & \text{in } \Omega \quad (9e) \\ \mathbf{c} = \mathbf{c}_\Gamma & \text{on }]0, T[\times \partial\Omega_- \quad (9f) \\ \mathbf{u} = \mathbf{u}_\Gamma & \text{on }]0, T[\times \partial\Omega \quad (9g) \end{array} \right.$$

One can verify that c has the same derivative as τ , leading to the new elastic transport equation

$$\lambda \frac{\mathcal{D}_a \boldsymbol{\tau}}{\mathcal{D}t} + \boldsymbol{\tau} - 2\eta_m D(\mathbf{u}) = \lambda \frac{\mathcal{D}_a \mathbf{c}}{\mathcal{D}t} + \mathbf{c} - \frac{\eta_m}{a\lambda} \mathbf{I}$$

3.2 Logarithm of the conformation tensor formulation

3.2.1 The change of variable

We now introduce the logarithm $\boldsymbol{\chi}$ of the conformation tensor \boldsymbol{c} from [6] :

$$\boldsymbol{\chi} = \frac{\eta_m}{a\lambda} \log \left(\frac{a\lambda}{\eta_m} \boldsymbol{c} \right) \Leftrightarrow \boldsymbol{c} = \frac{\eta_m}{a\lambda} \exp \left(\frac{a\lambda}{\eta_m} \boldsymbol{\chi} \right). \quad (10)$$

To perform such change of unknown, we have to write the constitutive equation on the eigenbasis, where \boldsymbol{c} is diagonal. Then perform the change of unknown and finally perform the change of basis from the eigenbasis to the usual one. All those steps can be found in the book [7] from P.Saramito. We will now introduce the log derivative of a tensor.

3.2.2 The log derivative of a tensor

Before the introduction of the log derivative of a tensor, we define some tools that will be used later. Let us consider a tensor $\boldsymbol{\beta} \in \mathbb{R}_s^{N \times N}$, then $\{\beta_i\}$, $i = 1, 2, \dots, N(\boldsymbol{\beta}) \leq N$ denotes the set of the distinct eigenvalues of $\boldsymbol{\beta}$, $m(\beta_i)$ is the multiplicity of the eigenvalue β_i and $\{u_j^i\}_{1 \leq j \leq m(\lambda_i)}$ are the eigenvectors associated to the eigenvalue β_i of $\boldsymbol{\beta}$.

Definition 3.1. A eigenprojector \boldsymbol{P}_i associated to the eigenvalue λ_i of a tensor $\boldsymbol{\beta}$ is defined by

$$\boldsymbol{P}_i(\boldsymbol{\beta}) = \sum_{j=1}^{m(\lambda_i)} u_j^i \otimes u_j^i.$$

Definition 3.2. Let $\boldsymbol{\beta}$ be a symmetric real tensor, then the spectral decomposition of $\boldsymbol{\beta}$ can be written :

$$\boldsymbol{\beta} = \sum_{i=1}^{N(\boldsymbol{\beta})} \beta_i \boldsymbol{P}_i \quad (11)$$

where β_i , $i = 1, 2, \dots, d$ are the distinct eigenvalues of $\boldsymbol{\beta}$ and \boldsymbol{P}_i are as in definition 3.1.

We can now introduce the log derivative of a tensor:

Definition 3.3. The log derivative of a tensor $\boldsymbol{\chi}$ and $\boldsymbol{\gamma}$ is defined as

$$\frac{\mathcal{D}_{\log \boldsymbol{\chi}}}{Dt}(\boldsymbol{\chi}, \boldsymbol{\gamma}) = \dot{\boldsymbol{\chi}} + \boldsymbol{\chi} W(\boldsymbol{\gamma}) - W(\boldsymbol{\gamma}) \boldsymbol{\chi} + a \left(\boldsymbol{\chi} \tilde{W} \left(\frac{a\lambda}{\eta_m} \boldsymbol{\chi}, 2D(\boldsymbol{\gamma}) \right) - \tilde{W} \left(\frac{a\lambda}{\eta_m} \boldsymbol{\chi}, 2D(\boldsymbol{\gamma}) \right) \boldsymbol{\chi} \right) \quad (12)$$

where $\dot{\boldsymbol{\chi}}$ is the lagrangian derivative, $W(\boldsymbol{\gamma})$ is the skew symmetric part of $\boldsymbol{\gamma}$, $D(\boldsymbol{\gamma})$ is the symmetric part of $\boldsymbol{\gamma}$ and \tilde{W} is defined as

$$\tilde{W}(\boldsymbol{\beta}, \boldsymbol{\gamma}) = \sum_{i=1}^{N(\boldsymbol{\beta})} \sum_{j=1}^{N(\boldsymbol{\beta})} g \left(\frac{\beta_i - \beta_j}{2} \right) \boldsymbol{P}_i(\boldsymbol{\beta}) \boldsymbol{\gamma} \boldsymbol{P}_j(\boldsymbol{\beta})$$

with g defined as follow

$$g(x) = \begin{cases} \frac{1}{2x} - \frac{1}{2 \tanh x} & \text{if } x \neq 0 \\ 0 & \text{otherwise.} \end{cases} \quad (13)$$

The problem with the conformation tensor 9 becomes with the change of unknown 10:

Find $\boldsymbol{\chi}$, \mathbf{u} and p such that

$$\left\{ \begin{array}{ll} \operatorname{div} \mathbf{u} = 0 & \text{in }]0, T[\times \Omega \quad (14a) \\ \rho \left(\frac{\partial \mathbf{u}}{\partial t} + (\mathbf{u} \cdot \nabla) \mathbf{u} \right) - \operatorname{div} \left(\boldsymbol{\chi} + f \left(\frac{a\lambda}{\eta_m}, \boldsymbol{\chi} \right) + 2\eta_s D(\mathbf{u}) - p \mathbf{I} \right) = 0 & \text{in }]0, T[\times \Omega \quad (14b) \\ \lambda \frac{\mathcal{D}_{\log} \boldsymbol{\chi}}{\mathcal{D}t} + \boldsymbol{\chi} - f \left(\frac{a\lambda}{\eta_m}, \boldsymbol{\chi} \right) - 2\eta_m D(\mathbf{u}) = 0 & \text{in }]0, T[\times \Omega \quad (14c) \\ \boldsymbol{\chi}(t=0) = \boldsymbol{\chi}_0 & \text{in } \Omega \quad (14d) \\ \mathbf{u}(t=0) = \mathbf{u}_0 & \text{in } \Omega \quad (14e) \\ \boldsymbol{\chi} = \boldsymbol{\chi}_\Gamma = 0 & \text{on }]0, T[\times \partial\Omega_- \quad (14f) \\ \mathbf{u} = \mathbf{u}_\Gamma & \text{on }]0, T[\times \partial\Omega \quad (14g) \end{array} \right.$$

Theorem 3.1. *The change of unknown 10 transforms the problem 9 into 14.*

To begin the proof, we need to perform the change of unknown in the equation 9c:

$$\lambda \frac{\mathcal{D}_a \mathbf{c}}{\mathcal{D}t} + \mathbf{c} - \frac{\eta_m}{a\lambda} \mathbf{I} = 0$$

The computations are detailed in [7] and lead to:

$$\lambda \frac{\mathcal{D}_0 \boldsymbol{\chi}}{\mathcal{D}t} + \boldsymbol{\chi} - f \left(\frac{a\lambda}{\eta_m}, \boldsymbol{\chi} \right) + \eta_m \kappa \left(\frac{a\lambda}{\eta_m} \boldsymbol{\chi}, 2D(\mathbf{u}) \right) = 2\eta_m D(\mathbf{u}) \quad (15)$$

where

$$f(\mu, \boldsymbol{\chi}) \mapsto \begin{cases} \frac{\exp(\mu \boldsymbol{\chi}) - \mathbf{I}}{\mu} - \boldsymbol{\chi} & \text{if } \mu \neq 0 \\ 0 & \text{otherwise} \end{cases}$$

and $\kappa(\boldsymbol{\beta}, \boldsymbol{\gamma})$ is a function defined such that for all second order tensor $\boldsymbol{\beta} \in \mathbb{R}_s^{3 \times 3}$ and $\boldsymbol{\gamma} \in \mathbb{R}^{3 \times 3}$ we have:

$$\kappa(\boldsymbol{\beta}, \boldsymbol{\gamma}) = \mathbf{q}^T \tilde{\kappa} \mathbf{q}, \quad (16)$$

$$\tilde{\kappa}_{ij} = \hat{\kappa} \left(\frac{\beta_i - \beta_j}{2} \right) \tilde{\gamma}_{ij}, \quad 1 \leq i, j \leq d \quad (17)$$

$$\operatorname{diag}(\beta_i)_{1 \leq i \leq 3} = \mathbf{q}^T \boldsymbol{\beta} \mathbf{q} \quad (18)$$

$$(\tilde{\gamma}_{ij})_{1 \leq i, j \leq d} = \mathbf{q}^T \boldsymbol{\gamma} \mathbf{q} \quad (19)$$

$$\hat{\kappa}(x) = \begin{cases} 1 - \frac{x}{\tanh x} & \text{if } \mu \neq 0 \\ 0 & \text{otherwise} \end{cases} \quad (20)$$

The function κ is non linear with respect to its first argument making the derivatives hard to compute. We need an other expression.

Theorem 3.2. *The function κ can be rewritten in term of the spectral decomposition of its first argument $\boldsymbol{\beta}$:*

$$\kappa(\boldsymbol{\beta}, \boldsymbol{\gamma}) = \mathbf{q}^T \tilde{\kappa} \mathbf{q} = \sum_{i=1}^{N(\boldsymbol{\beta})} \sum_{j=1}^{N(\boldsymbol{\beta})} \hat{\kappa} \left(\frac{\beta_i - \beta_j}{2} \right) \mathbf{P}_i \boldsymbol{\gamma} \mathbf{P}_j \quad (21)$$

where \mathbf{P}_i and \mathbf{P}_j are eigenprojectors of $\boldsymbol{\beta}$ as defined in definition 3.1, $\tilde{\kappa}$ is as in equation (17), β_i are eigenvalues of $\boldsymbol{\beta}$ and \mathbf{q} is the 3×3 matrix whose i -th column is the eigenvector associated to β_i .

Proof. We start to develop from the third term in the equation (21) and decompose \mathbf{P}_i in the basis E_{ik} of the space $\mathcal{M}_n(\mathbb{R})$ where E_{ij} denotes the matrix equal to zero everywhere except at ij coordinate. The E_{ij} have the property that for all i, j, k, l :

$$E_{ij}E_{kl} = \delta_{jk}E_{il}$$

where δ_{ij} is equal to 0 if $i \neq j$. Let T be a matrix of $\mathcal{M}_3(\mathbb{R})$, then it admits a decomposition: $T = \sum_{i=1}^3 \sum_{j=1}^3 T_{ij}E_{ij}$ where T_{ij} is the number at the i -th row and j -th column.

This matrix decomposition leads to:

$$\begin{aligned} \sum_{i=1}^{N(\beta)} \sum_{j=1}^{N(\beta)} \hat{\kappa} \left(\frac{\beta_i - \beta_j}{2} \right) \mathbf{P}_i \boldsymbol{\gamma} \mathbf{P}_j &= \sum_{i=1}^{N(\beta)} \sum_{j=1}^{N(\beta)} \hat{\kappa} \left(\frac{\beta_i - \beta_j}{2} \right) \left(\sum_{m,m'}^N p_{mm'}^i E_{mm'} \right) \left(\sum_{n,n'}^N \gamma_{nn'} E_{nn'} \right) \left(\sum_{l,l'}^N p_{ll'}^j E_{ll'} \right) \\ &= \sum_{i=1}^{N(\beta)} \sum_{j=1}^{N(\beta)} \hat{\kappa} \left(\frac{\beta_i - \beta_j}{2} \right) \sum_{m,m',n,n'}^N p_{mm'}^i E_{mm'} \gamma_{nn'} E_{nn'} \left(\sum_{l,l'}^N p_{ll'}^j E_{ll'} \right) \\ &= \sum_{i=1}^{N(\beta)} \sum_{j=1}^{N(\beta)} \hat{\kappa} \left(\frac{\beta_i - \beta_j}{2} \right) \sum_{m,n,n'}^N p_{mn}^i \gamma_{nn'} E_{mn'} \left(\sum_{l,l'}^N p_{ll'}^j E_{ll'} \right) \\ &= \sum_{i=1}^{N(\beta)} \sum_{j=1}^{N(\beta)} \hat{\kappa} \left(\frac{\beta_i - \beta_j}{2} \right) \sum_{m,n,n',l,l'}^N p_{mn}^i \gamma_{nn'} E_{mn'} p_{ll'}^j E_{ll'} \\ &= \sum_{i=1}^{N(\beta)} \sum_{j=1}^{N(\beta)} \hat{\kappa} \left(\frac{\beta_i - \beta_j}{2} \right) \sum_{m,n,n',l'}^N p_{mn}^i \gamma_{nn'} p_{n'l'}^j E_{ml'} \end{aligned}$$

We now pose $l = n', l' = m', n = k'$ and $n' = k$ and rewrite p_{kj}^i in term of q . We have $P_i = \sum_{k=1}^{m(\lambda_i)} u_k^i \otimes u_k^i$, then $p_{jk}^i = (e_i \otimes e_i)_{jk} = e_j^i e_k^i$. As \mathbf{q} i -th column contains the eigenvector q_i associated to the eigenvalue β_i we have $p_{jk}^i = q_{ji} q_{ki}$. We insert this new expression and obtain:

$$\begin{aligned} \sum_{i=1}^{N(\beta)} \sum_{j=1}^{N(\beta)} \hat{\kappa} \left(\frac{\beta_i - \beta_j}{2} \right) \mathbf{P}_i \boldsymbol{\gamma} \mathbf{P}_j &= \sum_{i=1}^{N(\beta)} \sum_{j=1}^{N(\beta)} \hat{\kappa} \left(\frac{\beta_i - \beta_j}{2} \right) \sum_{m,m',k,k'}^N p_{mk'}^i \gamma_{k'k} p_{km'}^j E_{mm'} \\ &= \sum_{i=1}^{N(\beta)} \sum_{j=1}^{N(\beta)} \hat{\kappa} \left(\frac{\beta_i - \beta_j}{2} \right) \sum_{m,m',k,k'}^N q_{mi} q_{k'i} \gamma_{k'k} q_{kj} q_{m'j} E_{mm'} \\ &= \sum_{i=1}^{N(\beta)} \sum_{j=1}^{N(\beta)} \hat{\kappa} \left(\frac{\beta_i - \beta_j}{2} \right) \left(\sum_{k,k'}^N q_{k'i} \gamma_{k'k} q_{kj} \right) \left(\sum_{m,m'}^N q_{mi} E_{mm'} q_{m'j} \right) \end{aligned}$$

At this point the proof is done if we remark that:

$$\begin{aligned}
\tilde{\gamma}_{ij} &= (\mathbf{q}^T \boldsymbol{\gamma} \mathbf{q})_{ij} \\
&= \sum_{k=1}^N (\mathbf{q}^T \boldsymbol{\gamma})_{ik} q_{kj} \\
&= \sum_{k=1}^N \sum_{k'=1}^N q_{ik'}^T \gamma_{k'k} q_{kj} \\
&= \sum_{k,k'=1}^N q_{k'i} \gamma_{k'k} q_{kj}
\end{aligned}$$

and that :

$$\begin{aligned}
\mathbf{q} E_{ij} \mathbf{q}^T &= \left(\sum_{m,m'=1}^N q_{mm'} E_{mm'} \right) E_{ij} \left(\sum_{k,k'=1}^N q_{kk'}^T E_{kk'} \right) \\
&= \left(\sum_{m=1}^N q_{mi} E_{mj} \right) \left(\sum_{k,k'=1}^N q_{kk'}^T E_{kk'} \right) \\
&= \sum_{m,k,k'=1}^N q_{mi} q_{k'k} E_{mj} E_{kk'} \\
&= \sum_{m,k'=1}^N q_{mi} q_{k'j} E_{mk'}
\end{aligned}$$

By changing the index of the last sum: $k' = m'$, we can write

$$\mathbf{q} E_{ij} \mathbf{q}^T = \sum_{m,m'} q_{mi} q_{m'j} E_{mm'}$$

which leads to:

$$\begin{aligned}
\sum_{i=1}^{N(\boldsymbol{\beta})} \sum_{j=1}^{N(\boldsymbol{\beta})} \hat{\kappa} \left(\frac{\beta_i - \beta_j}{2} \right) \mathbf{P}_i \boldsymbol{\gamma} \mathbf{P}_j &= \sum_{i=1}^{N(\boldsymbol{\beta})} \sum_{j=1}^{N(\boldsymbol{\beta})} \hat{\kappa} \left(\frac{\beta_i - \beta_j}{2} \right) \left(\sum_{k,k'}^N q_{k'i} \gamma_{k'k} q_{kj} \right) \left(\sum_{m,m'}^N q_{mi} E_{mm'} q_{m'j} \right) \\
&= \sum_{i=1}^{N(\boldsymbol{\beta})} \sum_{j=1}^{N(\boldsymbol{\beta})} \hat{\kappa} \left(\frac{\beta_i - \beta_j}{2} \right) \tilde{\gamma}_{ij} \mathbf{q} E_{ij} \mathbf{q}^T \\
&= \mathbf{q} \left(\sum_{i=1}^{N(\boldsymbol{\beta})} \sum_{j=1}^{N(\boldsymbol{\beta})} \hat{\kappa} \left(\frac{\beta_i - \beta_j}{2} \right) \tilde{\gamma}_{ij} E_{ij} \right) \mathbf{q}^T \\
&= \mathbf{q} \left(\sum_{i=1}^{N(\boldsymbol{\beta})} \sum_{j=1}^{N(\boldsymbol{\beta})} \tilde{\kappa}_{ij} E_{ij} \right) \mathbf{q}^T \\
&= \mathbf{q}^T \tilde{\kappa} \mathbf{q} \\
&= \kappa(\boldsymbol{\beta}, \boldsymbol{\gamma})
\end{aligned}$$

□

We can now show the theorem 3.1, using the just shown theorem we can compute:

$$\begin{aligned}
\sum_{i=1}^{N(\boldsymbol{\beta})} \sum_{j=1}^{N(\boldsymbol{\beta})} \hat{\kappa} \left(\frac{\beta_i - \beta_j}{2} \right) \mathbf{P}_i \boldsymbol{\gamma} \mathbf{P}_j &= \sum_{i=1}^{N(\boldsymbol{\beta})} \sum_{j=1}^{N(\boldsymbol{\beta})} (\beta_i - \beta_j) g \left(\frac{\beta_i - \beta_j}{2} \right) \mathbf{P}_i \boldsymbol{\gamma} \mathbf{P}_j \\
&= \sum_{i=1}^{N(\boldsymbol{\beta})} \sum_{j=1}^{N(\boldsymbol{\beta})} \beta_i g \left(\frac{\beta_i - \beta_j}{2} \right) \mathbf{P}_i \boldsymbol{\gamma} \mathbf{P}_j - \sum_{i=1}^{N(\boldsymbol{\beta})} \sum_{j=1}^{N(\boldsymbol{\beta})} \beta_j g \left(\frac{\beta_i - \beta_j}{2} \right) \mathbf{P}_i \boldsymbol{\gamma} \mathbf{P}_j \\
&= \left(\sum_{l=1}^{N(\boldsymbol{\beta})} \beta_l \mathbf{P}_l \right) \sum_{i=1}^{N(\boldsymbol{\beta})} \sum_{j=1}^{N(\boldsymbol{\beta})} g \left(\frac{\beta_i - \beta_j}{2} \right) \mathbf{P}_i \boldsymbol{\gamma} \mathbf{P}_j - \\
&\sum_{i=1}^{N(\boldsymbol{\beta})} \sum_{j=1}^{N(\boldsymbol{\beta})} g \left(\frac{\beta_i - \beta_j}{2} \right) \mathbf{P}_i \boldsymbol{\gamma} \mathbf{P}_j \left(\sum_{l=1}^{N(\boldsymbol{\beta})} \beta_l \mathbf{P}_l \right) \\
&= \boldsymbol{\beta} \sum_{i=1}^{N(\boldsymbol{\beta})} \sum_{j=1}^{N(\boldsymbol{\beta})} g \left(\frac{\beta_i - \beta_j}{2} \right) \mathbf{P}_i \boldsymbol{\gamma} \mathbf{P}_j - \\
&\sum_{i=1}^{N(\boldsymbol{\beta})} \sum_{j=1}^{N(\boldsymbol{\beta})} g \left(\frac{\beta_i - \beta_j}{2} \right) \mathbf{P}_i \boldsymbol{\gamma} \mathbf{P}_j \boldsymbol{\beta} \\
&= \boldsymbol{\beta} \tilde{W}(\boldsymbol{\beta}, \boldsymbol{\gamma}) - \tilde{W}(\boldsymbol{\beta}, \boldsymbol{\gamma}) \boldsymbol{\beta}
\end{aligned}$$

And finally, substituting the newly found expression of kappa in the equation 15, we finish the proof of the theorem 3.1

$$\begin{aligned}
&\lambda \frac{\mathcal{D}_0 \boldsymbol{\chi}}{\mathcal{D}t} + \boldsymbol{\chi} - f \left(\frac{a\lambda}{\eta_m}, \boldsymbol{\chi} \right) + \eta_m \kappa \left(\frac{a\lambda}{\eta_m} \boldsymbol{\chi}, 2D(\mathbf{u}) \right) = \\
&\lambda \left(\dot{\boldsymbol{\chi}} + \boldsymbol{\chi} W - W \boldsymbol{\chi} + \frac{\eta_m}{\lambda} \left(\frac{a\lambda}{\eta_m} \boldsymbol{\chi} \tilde{W} \left(\frac{a\lambda}{\eta_m} \boldsymbol{\chi}, 2D(\mathbf{u}) \right) - \tilde{W} \left(\frac{a\lambda}{\eta_m} \boldsymbol{\chi}, 2D(\mathbf{u}) \right) \frac{a\lambda}{\eta_m} \right) + \boldsymbol{\chi} - f \left(\frac{a\lambda}{\eta_m}, \boldsymbol{\chi} \right) = \right. \\
&\lambda \left(\dot{\boldsymbol{\chi}} + \boldsymbol{\chi} W - W \boldsymbol{\chi} + a \left(\boldsymbol{\chi} \tilde{W} \left(\frac{a\lambda}{\eta_m} \boldsymbol{\chi}, 2D(\mathbf{u}) \right) - \tilde{W} \left(\frac{a\lambda}{\eta_m} \boldsymbol{\chi}, 2D(\mathbf{u}) \right) \boldsymbol{\chi} \right) \right) + \boldsymbol{\chi} - f \left(\frac{a\lambda}{\eta_m}, \boldsymbol{\chi} \right) = \\
&\lambda \frac{\mathcal{D}_{\log} \boldsymbol{\chi}}{\mathcal{D}t} (\boldsymbol{\chi}, 2D(\mathbf{u})) + \boldsymbol{\chi} - f \left(\frac{a\lambda}{\eta_m}, \boldsymbol{\chi} \right)
\end{aligned}$$

3.3 Abrupt contraction

In this section, we present a simulation of the flow of a viscoelastic fluid in planar abrupt contraction. The study of a viscoelastic flow in abrupt contraction has a direct industrial application in the making of wires. One of the main way to create a wire is to extrude a polymer solution, solidify the solution and wrap the obtained wire:

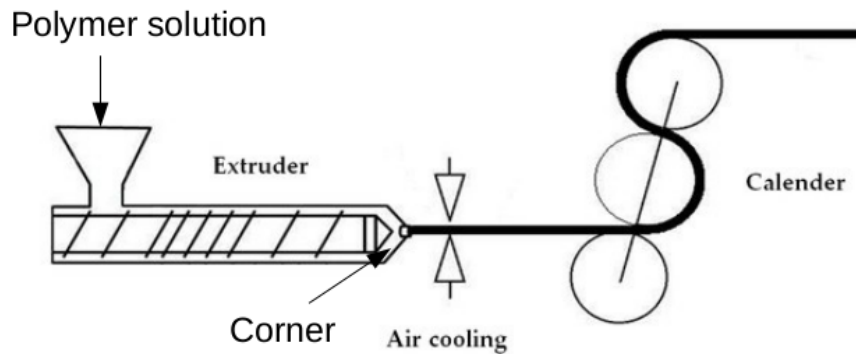


Figure 1: Scheme of a Industrial process to extrude a polymer material, figure taken from [3]

The main problem encountered in this process using polymers is that depending on the inflow speed and the Weissenberg number of the material a vortex is created around the corners of the extruder. This vortex will accumulate a lot of impurities during the process and at a certain time the vortex can move, we will use the term recirculate, from the corner to the output of the extruder and leak some impurities in the created wire. We will see later that the Weissenberg

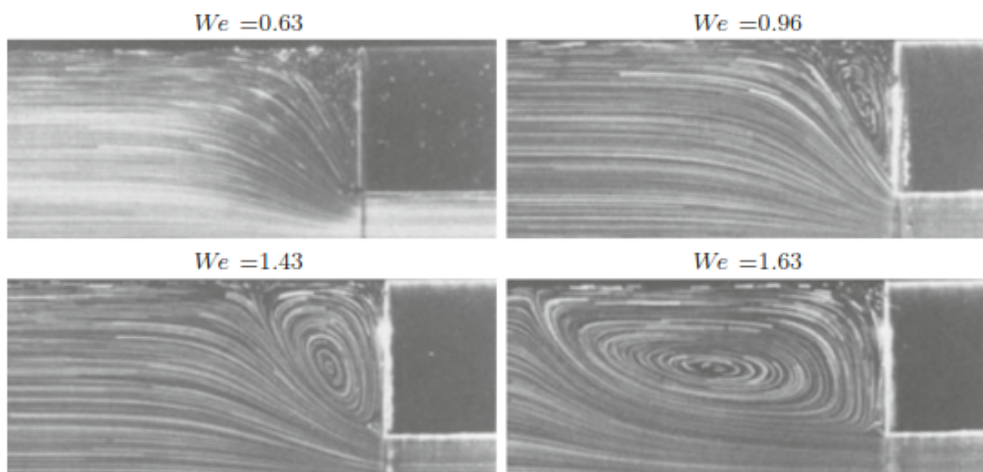


Figure 2: The creation of a vortex at different Weissenberg numbers, for an axis symmetric abrupt contraction, from [7]

number depends on three parameters: the relaxation time parameter λ that is characteristic to the material and the size of the extruder and the downstream speed of the flow that depend on the setup and the configuration of the extruder. In a pure industrial point of view, the

goal is to maximize the downstream speed to obtain a better productivity. By doing that, the Weissenberg number rise up and lead to a recirculation of the vortex inside the extruder and lead to the leak of impurities in the wire which is not acceptable. The goal of the presented simulation is to show the vortex behaviour at the corner for different Weissenberg numbers the intensity of the vortex and to compare the obtained results with those obtained by R.Comminal et al in [5]. All the simulations were done using the open source C++ library *Rheolef*.

3.3.1 Configuration

We choose the same configuration as the article [5]:

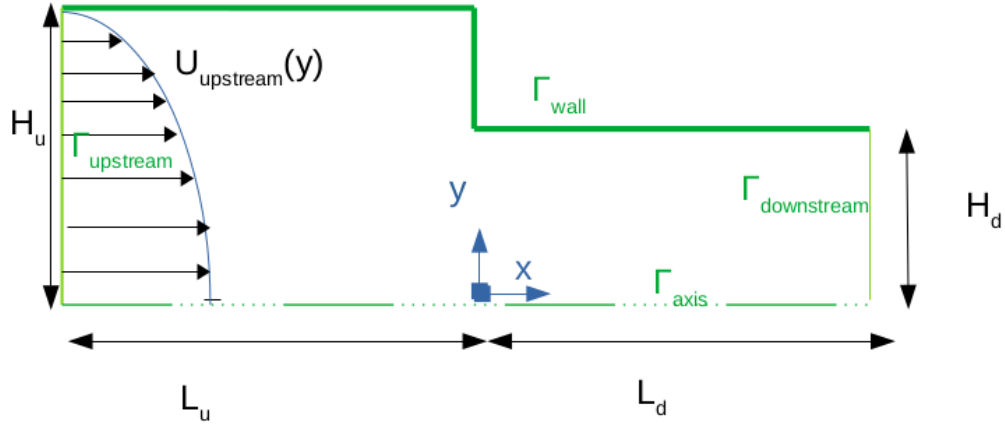


Figure 3: Abrupt contraction configuration

We define the contraction ratio c as the ratio between the upstream height H_u and of the downstream height H_d . The boundary conditions on $\mathbf{u} = (u_0, u_1)$ and χ are:

$$\begin{aligned} u_0 &= u_{upstream}(y) \text{ and } u_1 = 0 \text{ on } \Gamma_{upstream} \\ \mathbf{u} &= 0 \text{ on } \Gamma_{wall} \\ \sigma_{xx} &= 0 \text{ and } u_1 = 0 \text{ on } \Gamma_{downstream} \\ \sigma_{xx} &= 0 \text{ and } u_1 = 0 \text{ on } \Gamma_{axis} \\ \chi &= \chi_{upstream} \text{ on } \Gamma_{upstream} \end{aligned}$$

where $u_{upstream}(y) = U_{u,max}(1 - (2y/H_u)^2)$ with $U_{u,max}$ the maximal value of the inlet velocity.

To reduce the parameter set, let us perform a dimensional analysis, we denote by a tilde the dimensionless variables:

$$\tilde{x} = x/H_d \text{ and } \tilde{u}(x) = \frac{u(x)}{U_d} \text{ and } \tilde{\tau} = \frac{\tau}{\Sigma}$$

where U_d and Σ are respectively characteristic speed and characteristic deformation of the flow. The channels are chosen to be long enough such that the flow at the inlet and outlet behave as

in a poiseuil flow. In that condition, the tensor $\boldsymbol{\tau}$ verify:

$$\tau_{xy}(y) = \tau_{yx}(y) = -\alpha \frac{y}{H_u} \Sigma_u \quad (22)$$

$$\tau_{xx}(y) = (1 + a) We \alpha \left(\frac{y}{H_u} \right)^2 \quad (23)$$

$$\tau_{yy}(y) = -(1 - a) We \alpha \left(\frac{y}{H_u} \right)^2 \quad (24)$$

where $We = \lambda \frac{U_d}{H_d}$ is the Weissenberg number and $\alpha = \frac{\eta_m}{\eta_m + \eta_s}$ are dimensionless numbers. We choose for the abrupt contraction simulation the coefficient a equals to 1. $\boldsymbol{\chi}$ and $\boldsymbol{\tau}$ are linked by the logarithm of the conformation tensor formulation. We will normalize $\boldsymbol{\tau}$ first then explain all the step to obtain the normalization of $\boldsymbol{\chi}$.

The space variable x will be normalized with respect to the half-width H_d of the downstream channel. The variable U_d represents the average velocity of the flow at the downstream channel. We have:

$$\begin{aligned} \tilde{u}(\tilde{y}) &= \frac{u(H_d \tilde{y})}{U_d} \\ &= \frac{U_{u,max}}{U_d} \left[1 - \left(\frac{H_d}{H_u} \tilde{y} \right)^2 \right] \\ &= \frac{U_{u,max}}{U_d} \left[1 - \left(\frac{\tilde{y}}{c} \right)^2 \right] \end{aligned}$$

Let q be the flow rate of the fluid, it is equal to $U_d H_d$ at the downstream channel and $U_u H_u$ at the upstream channel. Mass conservation imposes q to be the same at the upstream channel and at the downstream channel which leads to the relation:

$$q = U_d H_d = U_u H_u \implies U_u = \frac{U_d}{c}.$$

We need to establish the link between U_d and $U_{u,max}$:

$$\begin{aligned} q &= \int_0^{H_u} U_d \tilde{u}(\tilde{y}) dy \\ &= \int_0^{H_u} U_{u,max} \left[1 - \left(\frac{\tilde{y}}{c} \right)^2 \right] dy \\ &= U_{u,max} \left[H_u - \frac{1}{c^2} \int_0^{H_u} \left(\frac{y}{H_d} \right)^2 dy \right] \\ &= U_{u,max} \left[H_u - \frac{1}{c^2 H_d^2} \frac{H_u^3}{3} \right] \\ &= U_{u,max} \left[H_u - \frac{H_u}{3} \right] \\ &= U_{u,max} \frac{2H_u}{3} \end{aligned}$$

Hence the relation between U_d and $U_{u,max}$:

$$U_u = \frac{2}{3}U_{u,max} \implies U_d = \frac{2c}{3}U_{u,max}$$

And finally the dimensionless velocity of the fluid is given by:

$$\tilde{u}(\tilde{y}) = \frac{3}{2c} \left[1 - \left(\frac{\tilde{y}}{c} \right)^2 \right] \quad (25)$$

We now normalize the stress tensor χ with respect to the downstream value Σ_d . Let Σ_d and Σ_u be:

$$\Sigma_d = (\eta_m + \eta_s) \frac{U_d}{H_d}$$

and:

$$\Sigma_u = (\eta_m + \eta_s) \frac{U_u}{H_u}$$

which leads to $\Sigma_u = \frac{1}{c^2}\Sigma_d$. The elastic stress tensor $\boldsymbol{\tau}$ is symmetric:

$$\begin{aligned} \tau_{xy}(y) = \tau_{yx}(y) &= -\alpha \frac{y\Sigma_u}{H_u} \\ &= -\alpha \frac{y}{H_u} \frac{\Sigma_d}{c^2} \\ &= -\frac{\alpha}{c^3} \Sigma_d \frac{y}{H_d} \end{aligned}$$

Hence

$$\tilde{\tau}_{xy}(\tilde{y}) = \tilde{\tau}_{yx}(\tilde{y}) = \frac{\tau_{xy}(\tilde{y})}{\Sigma_d} = -\frac{\alpha}{c^3} \tilde{y}$$

The xx component is given by:

$$\begin{aligned} \tau_{xx}(y) &= \Sigma_u 2\alpha We \left(\frac{y}{H_u} \right)^2 \\ &= \frac{1}{c^2} \Sigma_d 2We \left(\frac{y}{cH_d} \right)^2 \\ \tilde{\tau}_{xx}(\tilde{y}) &= \frac{2\alpha We \tilde{y}^2}{c^4} \end{aligned}$$

where We and α are defined above. To finish, we apply the change of variable. We introduce the conformation tensor $\mathbf{c} = \boldsymbol{\tau} + \frac{\eta_m}{a\lambda} \mathbf{I}$.

$$\tilde{\mathbf{c}} = \frac{\mathbf{c}}{\Sigma_d} = \tilde{\boldsymbol{\tau}} + \frac{\eta_m}{\lambda(\eta_m + \eta_s) \frac{U_d}{H_d}} \mathbf{I} = \tilde{\boldsymbol{\tau}} + \frac{\alpha}{We} \mathbf{I}$$

And finally the logarithm of the conformation tensor $\boldsymbol{\chi} = \frac{\eta_m}{a\lambda} \log\left(\frac{a\lambda}{\eta_m} \mathbf{c}\right)$ will be normalized as $\tilde{\boldsymbol{\chi}}$:

$$\tilde{\boldsymbol{\chi}} = \frac{\boldsymbol{\chi}}{\Sigma_d} \quad (26)$$

$$= \frac{\eta_m}{\lambda(\eta_m + \eta_s) \frac{U_d}{H_d}} \log\left(\frac{a\lambda}{\eta_m} \tilde{\mathbf{c}} \Sigma_d\right) \quad (27)$$

$$= \frac{\eta_m}{\lambda(\eta_m + \eta_s) \frac{U_d}{H_d}} \log\left(\frac{a\lambda}{\eta_m} c \Sigma_d\right) \quad (28)$$

$$= \frac{\alpha}{We} \log\left(\frac{We}{\alpha} \tilde{\mathbf{c}}\right) \quad (29)$$

3.3.2 Simulations

The simulation of a viscoelastic flow us a Newton algorithm implemented in *Rheolef* [8]. The simulations use a Euler-Newton continuation algorithm. It is a Newton method that allows to increase the Weissenberg number from the lowest value of the characteristic number, here equals to zero. At the lowest value of the Weissenberg number, the problem reduces to the Navier-Stoke problem. To fit the the R.Comminal *et al* results, we choose the value $\alpha = 8/9$, $c = 4$, $Lu = 24$ and $Ld = 20$. The result of the computation is the stationary solution of the problem 14. The continuation algorithm allowed us to push the simulation up to a Weissenberg number of 2.35 for the finest mesh and up to 2.7 for the coarsest mesh.

We used three differents meshes for the simulation:

Mesh	Number of triangles
m1	5634
m2	22584
m3	34941

Table 1: Meshes information

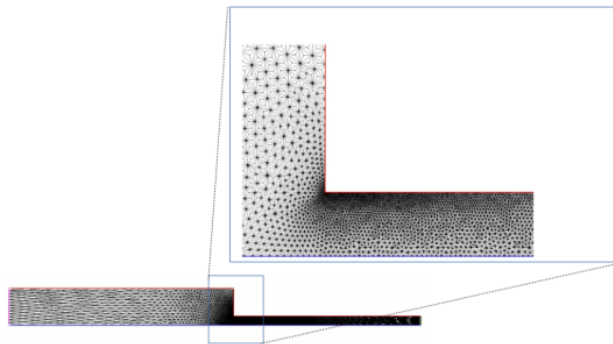
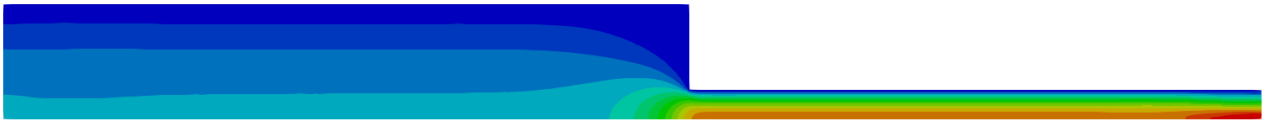


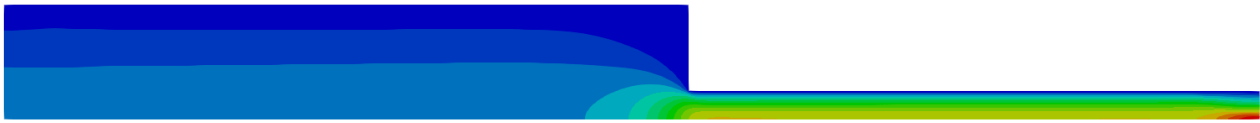
Figure 4: Illustration of the abrupt contraction mesh

The mesh is refined at the corner and at the entrance of the downstream channel, at this zone, the gradient of the velocity field has a skyrocketing norm and leads to inaccuracies in the computation.

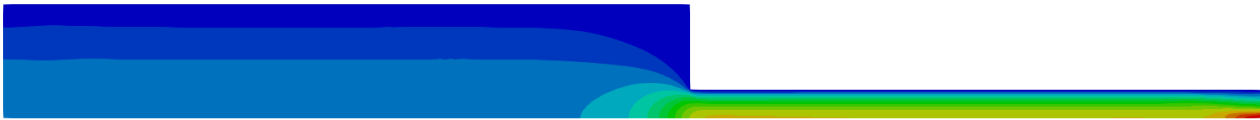
Let us observe the different results between the meshes, here for Weissenberg equal to one



(a) mesh m1



(b) mesh m2



(c) mesh m3

Figure 5: Velocity field for the abrupt contraction at Weissenberg equal to 1

At this Weissenberg, the velocity computation is not accurate for the mesh m1, the low number of elements in the mesh leads to inaccurate velocity field computation. Let us go to Weissenberg equals to two:

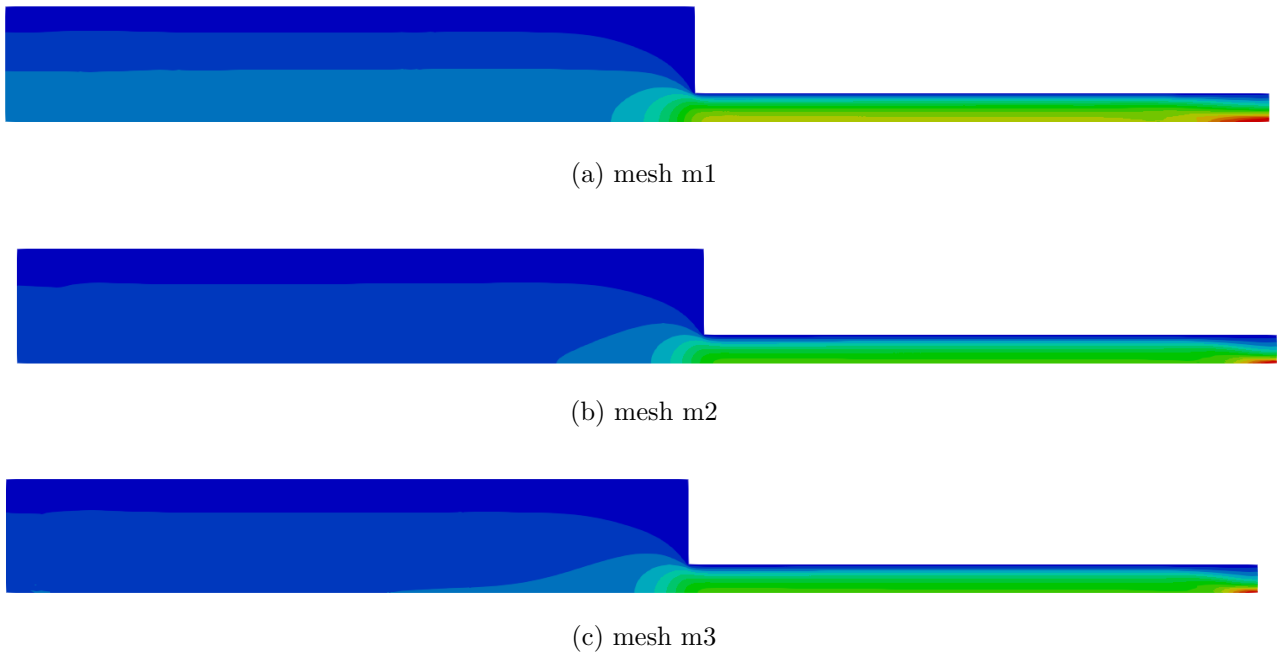


Figure 6: Velocity field for the abrupt contraction at Weissenberg equal to 2

At this point, we can not really interpret how the algorithm works and how the flow behaves at the corner. hence, we were interesting in computing the stream function ψ , a scalar valued field, see appendix B for the formula. This field is interesting in the study of a stationnary flow.

We present below the streamlines for some Weissenberg numbers obtained on the finest mesh m3.

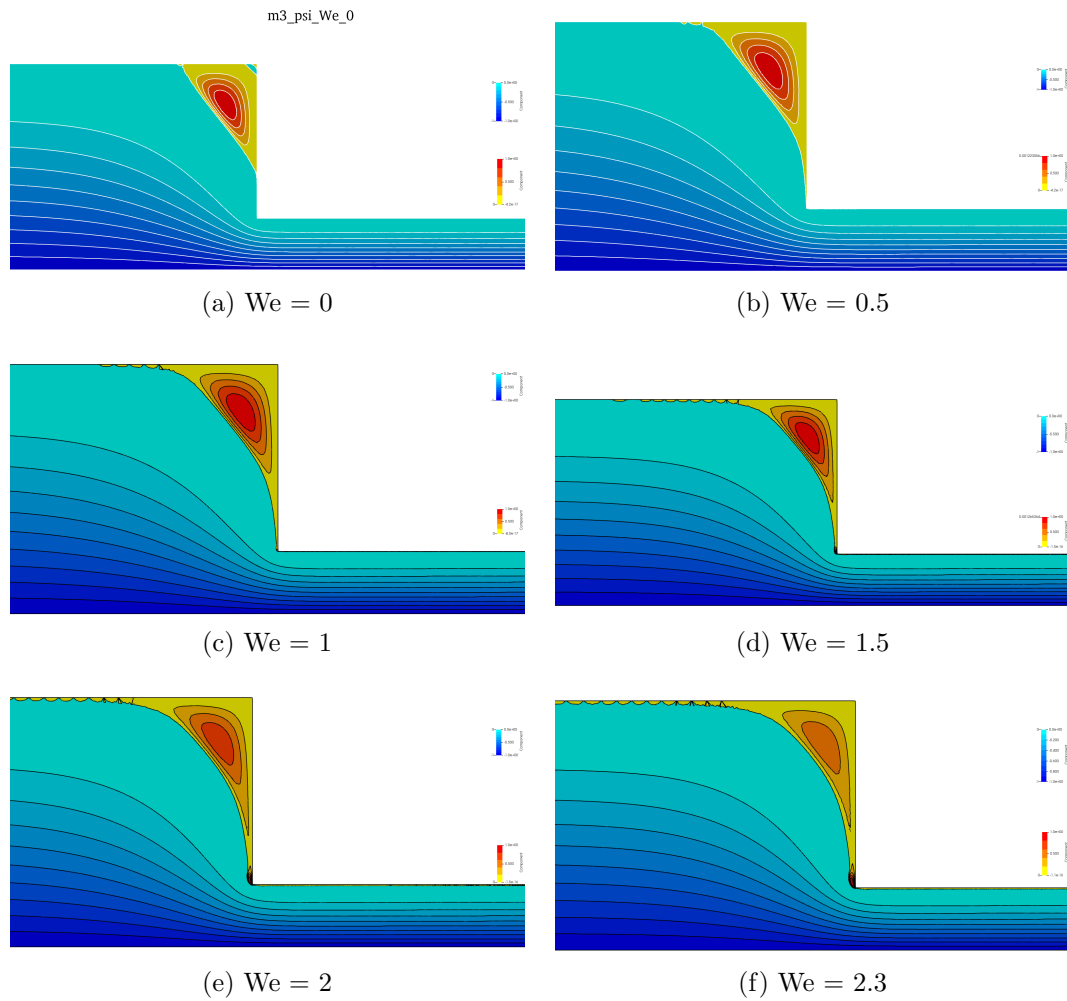


Figure 7: Streamlines for different Weissenberg number on the mesh m3

Those simulations gives us some information on the behaviour of the fluid. We can see that the corner vortex is loosing intensity while a new vortex is getting intensity at the edge of the entrance of the downstream channel, it is called the lip vortex. This behaviour is highlighted in R.Comminal *et al.* [5] and we can see it on the figure 7.f

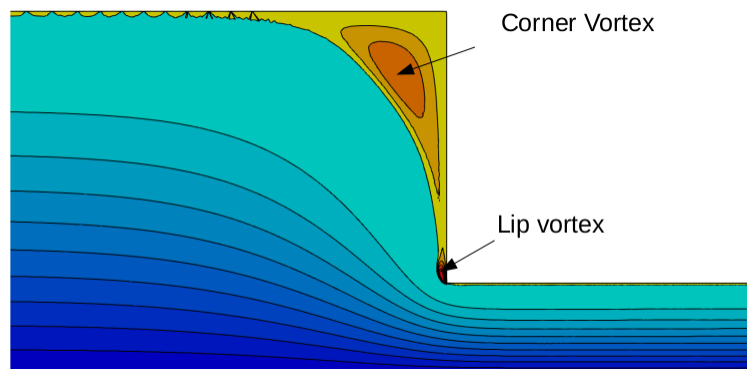


Figure 8: Illustration of the vortices at We =2.5 on m3

We can see that by increasing the Weissenberg number the corner vortex recirculate to create a lip vortex. To compare with the article [5], we computed the intensity of the corner vortex in function of the Weissenberg number, for values before $We = 1$:

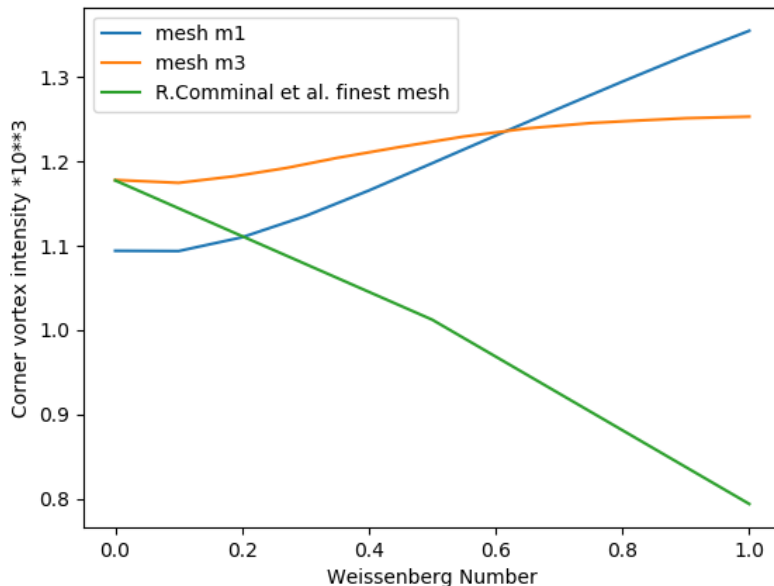


Figure 9: Intensity of the streamfunction at the corner in function of the Weissenberg number

Unfortunately, we did not achieve to the same intensity of the corner vortex as R. Comminal *et al* [5]. It seems that at Weissenberg equal to zero we have the same intensity but in their simulation the vortex intensity strictly decrease with the Weissenberg number. This can be linked with the computation of the ψ stream function that may be inaccurate.

At this point, we concluded that in term of recirculation our simulations agreed with the recirculations from R. Comminal *et al* [5]. They obtained a lip vortex at $We = 2$ too. Our main point of difference with the paper simulations is the evolution of the corner vortex intensity. Further investigations on the stream function may change that result.

4 Conclusion

This internship allowed me to put at work my skills in modelisation of complex physics phenomenon and to successfully illustrate some recent results on viscoelastic fluids.

I learned how to write the constitutive equations of a viscoelastic fluid and how to change the viscoelastic problem in term of the logarithm of the conformation tensor. In a second time, I rewrote the functions that appear in the logarithm of conformation change of unknown in term of them spectral decomposition. It allowed me to see the importance of some classic mathematics results such as the exponential of matrices, tensor equations or the derivative of a tensor. Then, I coded in *Rheolef* those functions from Appendix A for latter use during the internship. Those newly coded functions are supposed to replace the existing functions that are generated by a Computer Algebra System, Maxima.

This new approach developed during the internship of the viscoelastic problem allowed us to write a Newton algorithm in C++ with the library *Rheolef* to obtain the stationary solution of a viscoelastic flow in abrupt contraction. Although the results differed from the R.Cominal *et al* [5] for the intensity of the corner vortex, the simulation part was interesting for me to understand how it is to compare results from a personal work to a scientific publication. Even if my personal computer has a good processor allowing me to use mpi with six cores, simulations at high Weissenberg number can not be achieved after $We = 2.7$ without inaccuracies. An interesting continuation to the internship is the development of a Keller method that is an algorithm that allows to exceed the limit Weissenberg number, here $We = 2.7$.

A Computation of special functions

In that section, we define the functions we will use to solve the viscoelastic problem 14. To solve the viscoelastic problem 14 we use a Newton algorithm that relies on the computation of derivatives of the function f and of the log derivative.

A.1 Exponential of a tensor

Let \mathbf{T} be a real symmetric tensor, in [1], the exponential of \mathbf{T} can be computed by the explicit formula:

$$e^{\mathbf{T}} = \sum_{i=1}^d e^{\lambda_i} \mathbf{P}_i(\mathbf{T}),$$

where \mathbf{P}_i is the eigenprojector of \mathbf{T} as defined in definition 3.1 and λ_i are eigenvalues of \mathbf{T} .

A.2 Derivatives of the exponential of a tensor

Definition A.1. Let \mathbf{A} , \mathbf{B} be two tensors, we define the following square product of \mathbf{A} and \mathbf{B} by:

$$(\mathbf{A} \boxtimes \mathbf{B})_{ijkl} = \mathbf{A}_{ik} \mathbf{B}_{jl}.$$

Let \mathbf{T} be a real symmetric tensor, in [1], the derivative of the exponential of the tensor \mathbf{T} can be computed by the explicit formula:

$$\frac{\partial e^{\mathbf{T}}}{\partial \mathbf{T}} = \sum_{i=1}^d e^{\lambda_i} \mathbf{P}_i \boxtimes \mathbf{P}_i + \sum_{i=1}^d \sum_{j=1}^d \frac{e^{\lambda_i} - e^{\lambda_j}}{\lambda_i - \lambda_j} \mathbf{P}_i \boxtimes \mathbf{P}_j$$

where \mathbf{P}_i and \mathbf{P}_j are the eigenprojectors of \mathbf{T} as defined in definition 3.1 and λ_i , λ_j are eigenvalues of \mathbf{T} .

A.3 Derivative of the function kappa

In [2], an explicit formula of the derivative of kappa function with respect to the first argument is given:

$$\frac{\partial \kappa}{\partial \chi}(\chi, \gamma) = \sum_{i,j,k=1}^d \frac{\hat{\kappa}(\frac{\chi_i - \chi_k}{2}) - \hat{\kappa}(\frac{\chi_j - \chi_k}{2})}{\chi_i - \chi_j} \mathbf{P}_i \boxtimes \mathbf{P}_k \gamma \mathbf{P}_j + \mathbf{P}_k \gamma \mathbf{P}_j \boxtimes \mathbf{P}_i$$

where $\hat{\kappa}$ is defined in 20. If i and j coincide, then replace the scalar term of the sum by $\hat{\kappa}'(\chi_i - \chi_k)$.

B Computation of the stream function

We used the stream function definition from *Rheolef* [8]. Let \mathbf{u} be the velocity field of the problem 14, the stream function ψ is a scalar valued field that verifies the following system of equations

$$\begin{aligned} \Delta \psi &= \text{curl } \mathbf{u} \text{ in } \Omega, \\ \psi &= 0, \text{ in } \Omega. \end{aligned}$$

References

- [1] C.S. Jog. Derivatives of the stretch, rotation and exponential tensors in n-dimensional vector spaces. *Journal of Elasticity*, (82):175–192, 2006.
- [2] Philipp Knechtges. The fully-implicit log-conformation formulation and its application to three-dimensional flows. *Journal of Non-Newtonian Fluid Mechanics*, (223):209–220, 2015.
- [3] Amir Saffar Abdellah Aji Antonio B. Martínez David Arencón Pilar Castejón, Kian Habibi. Polypropylene-based porous membranes: Influence of polymer composition, extrusion draw ratio and uniaxial strain. https://www.mdpi.com/polymers/polymers-10-00033/article_deploy/html/images/polymers-10-00033-g001-550.jpg.
- [4] Raz Kupferman Raanan Fattal. Constitutive laws for the matrix-logarithm of the conformation tensor. *Journal of Non-Newtonian Fluid Mechanics*, (123):281–285, 2004.
- [5] Manuel A.Alves Jon Spangenberg Raphaël Comminal, Jesper H.Hattel. Vortex behavior of the oldroyd-b fluid in the 4-1p lanar contraction simulated with the streamfunction–log-conformation formulation. *Journal of Non-Newtonian Fluid Mechanics*, (237):1–15, 2016.
- [6] Pierre Saramito. On a modified non-singular log-conformation formulation for Johnson–Segalman viscoelastic fluids. *Journal of Non-Newtonian Fluid Mechanics*, (211):16–30, 2014.
- [7] Pierre Saramito. *Complex fluids: modeling and algorithms*. Springer, 2016.
- [8] Pierre Saramito. *Efficient C++ finite element computing with Rheolef*. version 7.1 update 22 March 2020, 2020.